

DOI: <http://doi.org/10.52716/jprs.v15i3.920>

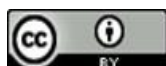
Detection Injection Zones in Carbonate Reservoir by Integration Production Log with Borehole Image Data at Horizontal Wells

Arab A. Albaaj, Basheer H. Murzooq, Maher J. Ismail, Rafea A. Abdullah*, Ahmed Saadoon

Ministry of Oil, Basra Oil Company, Basra, Iraq.

*Corresponding Author E-mail: raf32005@yahoo.com

Received 04/02/2024, Revised 22/06/2025, Accepted 29/06/2025, Published 21/09/2025

This work is licensed under a [Creative Commons Attribution 4.0 International License](https://creativecommons.org/licenses/by/4.0/).

Abstract

The Mid-Cretaceous Formation is a significant carbonate reservoir primarily located in the Middle East, notably in Iraq, Iran, and parts of the Arabian Gulf. It dates from the Late Cenomanian to Early Turonian period (94–90 million years ago). The formation comprises diverse lithologies, including bioclastic and rudist-rich limestone, grey-white limestone, foraminiferal-rich facies, and limonitic limestone. This study investigates the relationship between open-hole log data and dynamic injection data. The PoreSpect technique assumes that resistivity data from electrical borehole images reflect the flushed zone around the borehole. These electrical images, acquired using the Full-bore Formation MicroImager (FMI*), are calibrated with shallow resistivity and log-derived porosity to produce an effective porosity map. The underlying principle is that the FMI images provide a conductivity map of the borehole wall, which can be converted into porosity values using Archie's equation for the flushed zone. Image log interpretation provides valuable insights into porosity types and distributions. Primary porosity is associated with depositional processes, while secondary porosity—such as fractures and vugs—is developed through diagenetic alterations and is typically irregular in nature. This study focuses on the behaviour of the injection profile along the lateral section of horizontal wells, using image-derived porosity and logging-while-drilling density data. The findings reveal two distinct porosity groups. The first group, characterized by high secondary porosity (greater than 5%), accounts for over 90% of the injected water. The second group, despite having good total porosity, shows low secondary porosity and accommodates less than 10% of the injected water. A strong correlation exists between secondary porosity distribution and the injection profile, where zones with higher secondary porosity exhibit higher injectivity. Conversely, zones with high resistivity are associated with low injectivity and minimal secondary porosity. The approach presented in this study enhances the understanding of how different forms of carbonate porosity influence injection behaviour. The results confirm that secondary porosity plays a more significant role in injectivity than primary porosity. Although limited by the availability of horizontal production logging tool (PLT) data in injector wells, the analysis provides meaningful insights into injection performance.

These findings are essential for optimizing well completions, hydraulic fracture stage design, packer and inflow control device placement, and overall reservoir management strategies.

Keywords: borehole image, injection, primary porosity, secondary porosity.

تحديد انطقة الحقن في مكامن الكربونيت من خلال استخدام بيانات مجسات الانتاج مع مجس الامج في الابار الافقية

الخلاصة

تُعد تكوينات العصر الطباشيري الأوسط من المكامن الكربوناتية المهمة، وتقع بشكل رئيسي في منطقة الشرق الأوسط، ولا سيما في العراق، إيران، وأجزاء من الخليج العربي. ويعود تاريخها إلى الفترة الممتدة من السينوماني المتأخر إلى التوروني المبكر (منذ 94 إلى 90 مليون سنة). تتكون هذه التكوينات من مجموعة متنوعة من الصخور، تشمل الحجر الجيري البيوكلاستي والمحتوي على الروديست، والحجر الجيري الأبيض الرمادي، والواجهات الغنية بالفرامينيفيرا، والحجر الجيري الحاوي على الليمونيت.

تهدف هذه الدراسة إلى تحليل العلاقة بين مجس الآبار المفتوحة (Open-hole logs) والمجسات المبطنة الخاصة بالحقن. تعتمد تقنية PoreSpect على فرضية أن بيانات المقاومة الناتجة من صور الجدار البئري الكهربائية تمثل منطقة الغسل حول البئر. تُلتقط هذه الصور الكهربائية باستخدام جهاز التصوير الشامل لجدار التكوين (FMI*)، ثم تُعابر باستخدام المقاومة الضحلة وبيانات المسامية المشتقة من السجلات، لإنتاج خريطة للمسامية الفعالة. وتُبنى هذه الطريقة على أن صور FMI تمثل خريطة للتوصيلية الكهربائية لجدار البئر، والتي يمكن تحويلها إلى مسامية باستخدام معادلة آرثني لمنطقة الغسل. توفر تفسيرات صور السجل معلومات قيمة حول أنواع المسامية وتوزيعها. فالمسامية الأولية ترتبط بعمليات الترسيب، في حين أن المسامية الثانوية، مثل الشقوق والفرغات، تنشأ بفعل العمليات التحويرية وتتميز غالبًا بعدم انتظامها. تركز هذه الدراسة على سلوك ملف الحقن عبر القسم الأفقي للآبار الأفقية، من خلال استخدام المسامية المستخرجة من مجس الامج وبيانات الكثافة أثناء الحفر.

أظهرت النتائج وجود مجموعتين مميزتين من المسامية: المجموعة الأولى، التي تتميز بوجود مسامية ثانوية عالية (أكثر من 5%)، تمثل أكثر من 90% من حجم المياه المحقونة. أما المجموعة الثانية، فعلى الرغم من امتلاكها لمسامية كلية جيدة، إلا أن المسامية الثانوية فيها منخفضة، وقد استقبلت أقل من 10% من مياه الحقن. ويوجد ارتباط قوي بين توزيع المسامية الثانوية وملف الحقن؛ حيث أظهرت المناطق ذات المسامية الثانوية العالية معدلات حقن أعلى، بينما ارتبطت المناطق ذات المقاومة العالية بانخفاض قابلية الحقن وضعف في المسامية الثانوية.

تعزز هذه الدراسة فهم العلاقة بين أنواع المسامية الكربوناتية وسلوك الحقن. وتؤكد النتائج أن للمسامية الثانوية دورًا أكبر في قابلية الحقن مقارنة بالمسامية الأولية. ورغم محدودية توفر بيانات أداة تسجيل الإنتاج الأفقية (PLT في آبار الحقن، فإن التحليل يقدم رؤى مهمة حول أداء الحقن. تُعد هذه النتائج ضرورية لتحسين تصميم إكمال الآبار، وتحديد مراحل التكسير الهيدروليكي، ومواقع تثبيت الحواجز وأجهزة التحكم بالتدفق، وتحقيق إدارة أفضل للمكامن.

1. Introduction

The Mid-Cretaceous Formation is a large carbonate reservoir formation located largely in the Middle East, particularly in Iraq, Iran, and sections of the Arabian Gulf region. It dates from the Late Cenomanian to Early Turonian epoch (about 94-90 million years ago). The formation is mostly composed of limestone, frequently chalky or reef, with dolomite, marls, and shales in certain locations. The porosity at the formation is a varies types (moldic, vuggy, intercrystalline) which mostly classified as secondary porosity [1]. The investigated formation, which has about

30% of Iraq's oil reserves, is the most significant carbonate reservoir in the country [2]. The formation was deposited during the Middle Cenomanian to Early Turonian age, when thick carbonate sequences accumulated across a shallow, basin-wide platform [3]. The lithology of the study formation comprises various types, including bioclastic, rudist, grey-white limestone, foraminiferal-rich facies, and limonitic limestone [3]. The habitats of the studied formation gradually change from mid-ramp to lagoonal supratidal settings, consistent with the carbonate ramp model, which suggests that shallow waters are cyclically favorable for carbonate deposition [4].

Microresistivity imaging technologies were first introduced in the 1980s. The four-arm dipmeter tool was the first imaging device, originally adapted from wireline density skid technology [5]. The four-arm dipmeter instrument consists of two sensors on two arms and two imaging sensors on the other two arms [6]. Schlumberger's Formation Micro Scanner (FMS) began with capturing borehole images but was later transformed into a four-arm imaging instrument. Imaging tools underwent significant advancements in the early 1990s. Oil service businesses began to significantly enhance borehole coverage and resolution [7]. Schlumberger's FMI tool, Baker Hughes' STAR tool, Halliburton's EMI tool, and Weatherford's HMI tool (Weatherford, 2007) are among the most regularly used tools [8]. The current imaging instruments are made up of four, six, or eight hydraulically articulated arms that work in tandem with four, six, or eight sets of main and articulated pads to provide varying percentages of borehole coverage. When the hole size rises, the percentage coverage of the borehole wall falls in all image logging techniques. The depth of inquiry (DOI) for all tools was around 5 cm (2 in.) or less [9]. The imaging instruments may respond to deeper signals, such as current flowing from the tool pad to the mandrel, based on the formation's resistivity and the contrast of resistivity over the measured interval. Limitations in telemetry capabilities have restricted the number of measurements that imaging tools can transmit. The surface acquisition system acquired this vast amount of data via the telemetry systems, which improve with time and increase the number of measurements downhole [10]. The FMI instrument is supported by four main pads and four subsidiary pads, known as flaps. These eight pads, or flaps, are made up of two rows of 12 buttons, yielding 192 sensor electrodes. To offer enough coverage, the buttons on microresistivity imagers are positioned in two rows with a 50% overlap. They have a vertical resolution of 0.2 inch (5 millimeters). Submillimeter fractures, for example, can be recognized with a vertical resolution considerably lower than the tools, although assessment

of these characteristics requires a supplementary calculation. Figure (1) illustrates the measurement principle and design of the FMI tool (Figure 1).

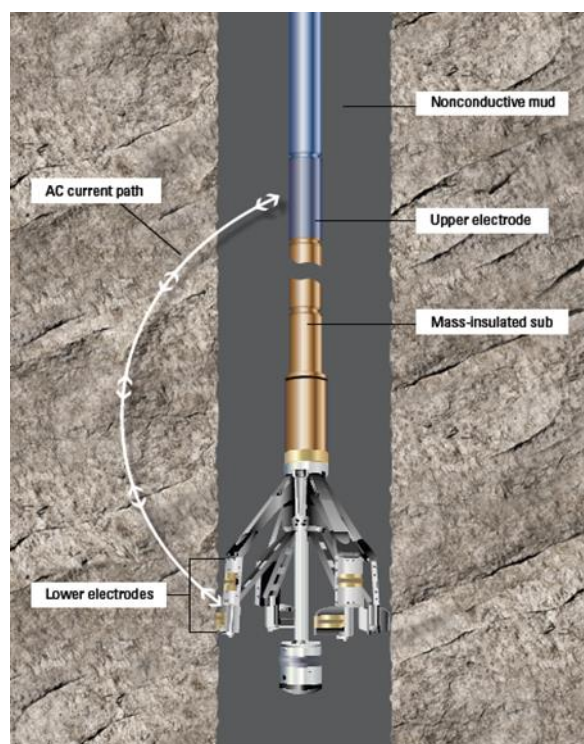


Fig. (1): FMI logging tool

Borehole image logs can be used to directly analyze sedimentary reservoir parameters [8]. The challenge is in developing diagnostic standards for classifying image log facies and translating image logs into sedimentary and structural characteristics such as sedimentary structures, bedding sequences, vertical grain-size successions, fractures, and in situ stress orientation [6]. Borehole image log facies refer to visual features identified through color variations in static images and dip patterns represented by sine waves in dynamic images. Some of the criteria used to interpret the picture facies include color variation patterns, imaging of sedimentary textures and structures, and structural elements on images [11]. Fine sedimentary reservoir features such as lithology, sedimentary structures, depositional microfacies, faults, fractures, and paleocurrent direction may therefore be determined using borehole image facies analysis. This study creates a total of five descriptive, easy-to-understand, and brief picture log facies that have been analyzed from both publicly available studies and peer-reviewed literature [12].

High resolution and azimuthal borehole coverage are provided by borehole electrical images, and FMI in particular enables the quantitative resolution of the heterogeneous character of porosity components. The use of borehole electrical pictures in the investigation of the carbonate reservoir porosity system has been made possible by the introduction of this strategy [13] [14]. This method may be used to determine the porosity distribution and volume of the vugs-modal fraction. However, shale and bad-hole conditions have a significant impact on the technique's performance. Images that have a damaged FMI pad or a poor hole that significantly impairs one or two pictures' quality might be rejected during analysis.

The most recent addition to the basket offers outputs at wireline-par resolution: the new generation ultra-high resolution LWD imager (Figure 2). Currently, there is better confidence in the interpretation of characteristics when using extra-high-quality images. Previously only possible with wireline pictures, custom software plug-ins are now readily accessible to even undertake quantitative analysis of these images (secondary porosity, fracture characteristics extraction/estimate).

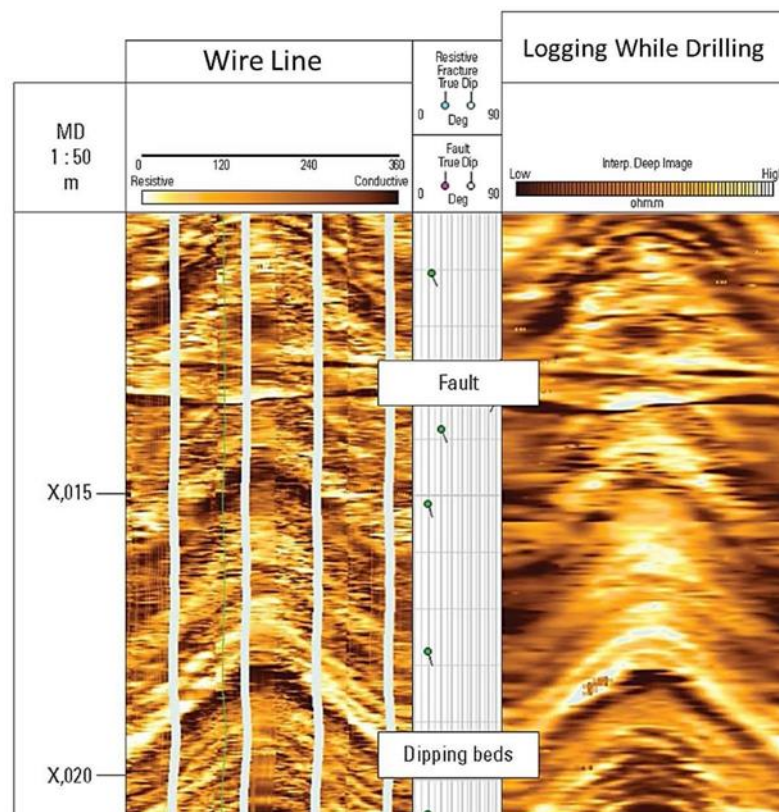


Fig. (2): Comparison of the Wire Line Resistivity Image with the LWD Resistivity Image

Injection zones tend to have higher permeability compared to adjacent areas; the main challenge lies in understanding the injection mechanism in horizontal wells. Horizontal wells are typically drilled within homogeneous layers characterized by similar rock properties. Due to high heterogeneity at the studied formation and to more understanding for the injection zones and the relationship between the secondary porosity that caused by diagenesis processing and the injection zones. For many years, the PLT has been utilized to diagnose production issues and do reservoir studies. With mature reservoir capacity falling and their shift towards secondary recovery, the need for production logs is growing. Their use is regarded as critical for understanding production behavior and selecting appropriate approaches for maximizing productivity and hydrocarbon recovery. Production logging (PLT) is used to diagnose a range of production issues as well as to evaluate reservoirs. The principal use of PLT is the detection of water ingress into producing wells. When the flow velocity of the water is low, the sensitivity of PLT prevents effective characterization. Water flooding, or waterflood, is a common technique used in the oil and gas industry to enhance oil recovery from reservoirs. The primary objective of water injection is to maintain reservoir pressure and displace additional oil towards production wells, ultimately increasing the overall recovery factor. a summary of how water injection in petroleum wells works: Maintaining reservoir pressure.

The pressure in a petroleum reservoir decreases over time as oil is extracted from it. This drop in pressure may result in reduced oil production rates and a slower total recovery. Water injection is the process of injecting water into a reservoir in order to maintain or raise reservoir pressure. This helps direct the leftover oil to the producing wells. Sweep Efficiency: Oil does not flow evenly through the rock formation when it is extracted from a reservoir. The fluids in the reservoir may bypass some regions of the reservoir. To "sweep" through these omitted regions and move the residual oil into producing wells, water is injected. This raises recovery efficiency as a whole. Viscosity Reduction: Over time, the oil in many reservoirs thickens and becomes more viscous as a result of variables including temperature variations and fluid interactions inside the reservoir. Water injection can aid in lowering the viscosity of the oil, facilitating flow to the producing wells. Dedicated Injection and Production Wells: A typical water injection project includes the drilling of dedicated injection and production wells. Injection wells are used to inject water into the reservoir, while production wells are used to recover the oil and water combination produced by the injection process. While water injection is a beneficial approach for improving oil recovery,

its effectiveness is dependent on a variety of parameters, including reservoir characteristics, fluid properties, and overall injection process management. Water quality, injection rates, and pressure maintenance tactics are just a few of the factors that must be considered for an efficient water injection program.

2. Methodology

The (FMI) is a high-resolution borehole imaging equipment used in well logging to examine geological formations. It generates precise resistivity-based pictures of the borehole wall, allowing geologists and engineers to evaluate structural and sedimentary aspects. Azimuthal Resolution: The FMI tool has an azimuthal resolution of 192 pixels, which allows for detailed imaging of the borehole wall. Vertical Resolution: To ensure that fine-scale geological features are recorded, the vertical resolution is 0.2 inches with a vertical sample interval of 0.1 inches. Depth of examination: The instrument is useful for examining near-wellbore formations since it measures microresistivity with a depth of examination of around 5 mm.

The data of FMI calibration included Software Calibration: Utilize software tools provided by the imager manufacturer to calibrate the data. This may involve applying correction factors to the raw data. Image Processing: Process the images to enhance quality and ensure accurate representation of the borehole wall. Understanding primary and secondary porosity is critical for evaluating subsurface reservoirs while doing formation evaluation with a Full-bore microresistivity Imager (FMI). Here is a discussion of these principles and how they apply to FMI data. FMI in evaluating porosity. The Fullbore Microresistivity Imager generates high-resolution pictures of the borehole wall as well as comprehensive resistivity data that may be utilized to study both primary and secondary porosity. Image Interpretation: FMI produces precise photos of the borehole wall, allowing geoscientists to visually examine the rock's texture and structure. Fractures, vugs, and various porosity types can be determined from the images. Resistivity measurements: The resistivity of a rock might show its porosity levels. In general, greater resistivity levels indicate lower water saturation and maybe larger porosity. The resistivity response may be used to determine the existence of primary and secondary porosity.

Calibration of the Production Logging Tool (PLT) is necessary to ensure accurate fluid flow measurements in a wellbore. Calibration is setting the tool's sensors to match known reference values, hence increasing the accuracy of the data obtained. Ensures that sensors read zero when no flow is present. Uses controlled flow conditions to establish accurate response curves. Adjusts for

environmental variations affecting sensor accuracy. Ensures the spinner correctly measures fluid velocity.

The technique that uses for this study is process the image log data and generate three image types: static image, dynamic image and equal image. The equal image data is analyzing the histogram which can show the in Figure (3). Three types of histograms showed in histograms: uni-model that means the porosity just a primary porosity, bi-model which show the primary and secondary porosity and multi-model which refers to high heterogeneity in carbonate rocks. The Archie equation can be used to characterize fluid saturation by analyzing how electrical current flows through the conductive brine within the porous medium [15]. He determined that the rock's "formation factor," which is a characteristic, is a relationship between the rock and the fluid that saturates it but is mostly influenced by sorting and rock texture equation 1.

$$S_w^n = \frac{aR_w}{\Phi^m R_t} \quad (1)$$

Where:

S_w : Water saturation, fraction

n: Saturation exponent = 2

a: Empirical

constant = 1

m: Cementation exponent = 2

ϕ : Porosity

R_w : Resistivity of formation water

R_t : Resistivity of uninvaded formation

This method is based on the premise that resistivity data from electrical images represent the flushed zone of the borehole. After calibration, these electrical images are calibrated using shallow resistivity and log porosity data to generate a porosity map (ideally effective porosity). For these types of advances, equation (2) is employed; it accepts as inputs log porosity (with effective log porosity being the optimum choice), any shallow resistivity measurement (often LLS or SFLU), and the conductivity of each individual FMI electrode or button (C_i) [14].

$$(\Phi)_{FMI*/FMS} = (\Phi)_{log} * [LLS * C_i]^{1/m} \quad (2)$$

Φ = porosity

LLS= shallow resistivity measurement

C_i = constant (depends on lithology)

2.1. Porosity classification

In order to create a porosity map of the drill interior using electrical borehole photos, the authors in [14] developed a method they named PoroSpect. Their fundamental presumption was that the FMI* (Full-bore Formation Micro Imager) calibrated electrical pictures are essentially a conductivity map of the borehole wall, largely from inside the flushed zone. They applied the traditional Archie saturation calculation for the flushed zone to convert this conductivity map into a porosity map of the drill surface [10].

A probabilistic technique was applied using the full suite of logs from all wells to estimate the porosity spectrum in the study area. Where the log quality is low owing to the hole condition, the level of uncertainty increases. The primary reservoirs, where core porosity and interpretation log porosity are in excellent agreement, are fortunately rather certain [16]. When the log has not been gathered with adequate reading, especially in vugs, modals holes, and washed-out periods, the porosity should be utilized with caution. Based on core and FMI data, two broad categories of porosity, including micro-porosity or inter-crystalline and vugs porosity, are recognized.

An essential assumption in high-resolution porosity analysis from image logs is that the resistivity data represent the flushed zone of the borehole. After calibration with shallow resistivity and log porosity (in an ideal effective porosity), the electrical pictures are turned into a porosity map of the borehole. This porosity map's automated analysis, windowed at short intervals, provides a continuous output of the primary and secondary porosity components. Porosity distribution histograms are produced at each set sample rate (usually 0.6 inches). The porosity distribution of the homogeneous carbonate intervals is unimodal, whereas the porosity distribution of the vuggy intervals is bimodal. Trimodal porosity distributions can occur in intervals with exceptionally high heterogeneity. On the porosity histograms, the points at the high porosity ends reflect the vugs and fracture fraction of porosity, while the points near the low porosity ends represent thick or cemented regions of the host rock. The average image porosity should be the same as the effective log porosity over the homogeneous carbonate intervals with a unimodal porosity distribution, but the unimodal porosity distribution shifts to a bimodal or trimodal distribution over the heterogeneous carbonate intervals. Depending on the kind of heterogeneity, such as vugs, molds,

fractures, or patches of particularly dense or porous material, the average image porosity over such heterogeneous intervals may be greater or less than the effective log porosity Figure (3). When core data and results of the porosity derivate from the resistivity image are examined, it is clear that the resistivity image covers secondary as well as primary porosity because heterogeneous media are distributed differently than homogeneous media.

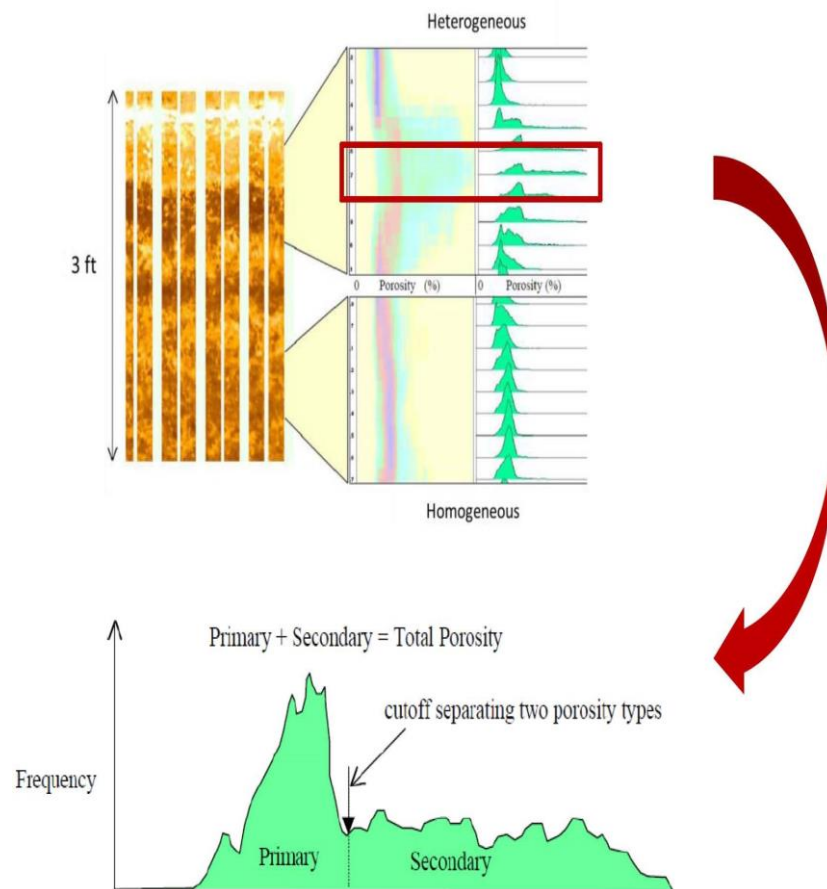


Fig. (3): The principle is to employ a cut-off to eliminate the secondary porosity component

2.2. Flow rate determination

The spinner rotation rate varies proportionally with the fluid flow rate. This relationship is generally linear for continuous flowmeters, including full-bore flowmeters, and generally non-linear for petal-basket flowmeters; thus, in single-phase flow (oil, gas, or water only), the flow profiling interpretation technique is essentially the plotting of spinner data in revolutions per second, such that the percentage flow contribution of each zone can be read directly from the plot (assuming fluid viscosity and density are covariant) [15]. The complexities of flow rate measurement in fluid dynamics, particularly in scenarios where fluid viscosity and density, alongside velocity, play crucial roles, Flow rate measurement is indeed influenced by various

factors, and your statement highlights the need for careful consideration when dealing with flowmeter data to obtain accurate results [17].

In situations where you want to determine absolute flow rates instead of just relative percentage contributions or when dealing with varying viscosity or density within a given interval, additional precautions are necessary. This holds true even in single-phase flow scenarios, where only one type of fluid is moving through the system.

One method mentioned for addressing these challenges is the use of downhole calibrations. Downhole calibrations involve performing measurements or adjustments directly in the environment where the fluid is flowing, typically within a wellbore or other confined spaces. In-situ calibrations account for specific fluid conditions—such as viscosity, density, and velocity—which may differ from standard flow assumptions Top of Form.

3. Results and Discussions

The current study included two horizontal wells (injector wells), and these well data were recorded using an LWD ultrahigh-resolution image logging tool. The borehole image is the main data used to determine the image porosity. The porosity partition uses the image scale technique called PoroSpect [4]. Primary and secondary image logs are types of well logs that provide information about the properties of subsurface formations. These logs are acquired through various tools that are lowered into a borehole to measure the different properties of the rocks. The table below show the relationship between the injection rate and the secondary porosity values even the total porosity values are closed each other. The injection rates are increased when the secondary porosity is increasing.

Table (1): Injection rate, total porosity & secondary porosity values for studied well

No.	Interval m	Injection rate bbl/day	porosity(pu)	Secondary porosity(pu)
1	3227-3250	-105	0.23	0.02
2	3310-3337	-65	0.22	0.01
3	3390-3423	-457	0.24	0.04
4	3470-3507	-1327	0.25	0.7
5	3517-3554	-3260	0.258	0.8

Depends on the data in this case study, the results are:

3.1. Good secondary porosity high injectivity zones

As the table above the injection zones 3&4 that refers to good rock properties with diagenesis processes as well as dissolution. Secondary porosity values range between 5 and 8 porosity units (pu). These two zones are taken more than 90% of injection water. In spite of the total porosity are closed to the total porosity that determine in low secondary porosity zones. The fact that there's a good agreement between the curves indicates that the porosity estimation process is reliable and accurate. Additionally, the presence of high secondary porosity within the interpreted vuggy zone is an interesting observation, as it suggests that this particular zone has undergone processes that have led to enhanced porosity in the surrounding rocks. The black curve likely represents porosity estimates derived from resistivity data. In geophysics, resistivity measurements can help differentiate between different rock types and their porosity, as different rocks have different electrical resistivity properties. The presence of high secondary porosity in the open fault zone, as indicated by the black curve, suggests that this vuggy zone is a favorable location for fluid accumulation and flow due to the increased pore space. The injectivity for these zones.

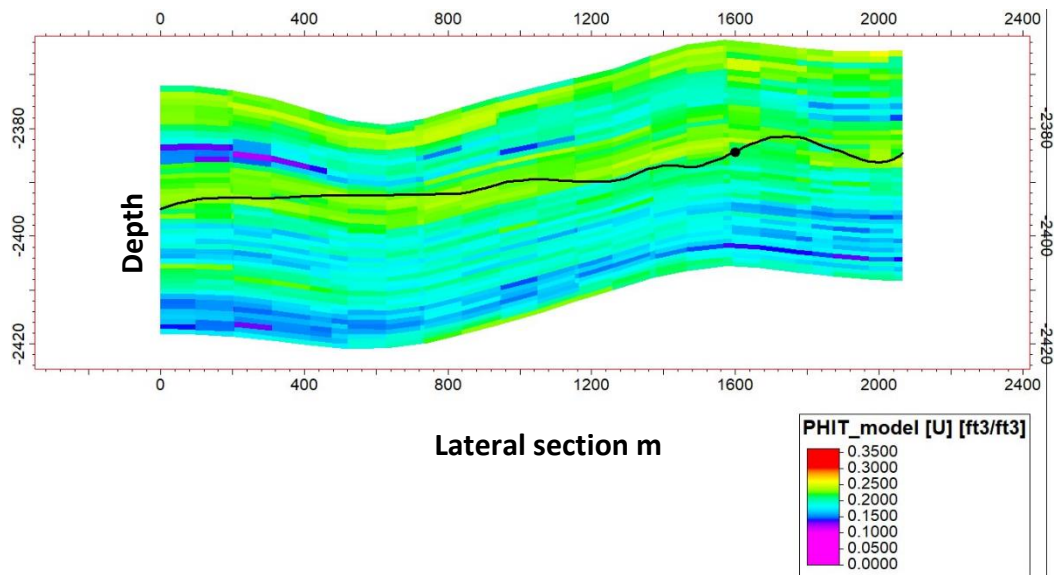


Fig. (4): study well porosity model

3.2. Low secondary porosity low injectivity zones

These zones have high primary porosity formed during deposition, while the secondary porosity—resulting from vugs and diagenetic dissolution—is less than 4 pu. The injectivity in

these zones shows a low spinner contribution and a low injection rate. The resistivity values show high values in the compact limestone microporous pores system (Figure 5).

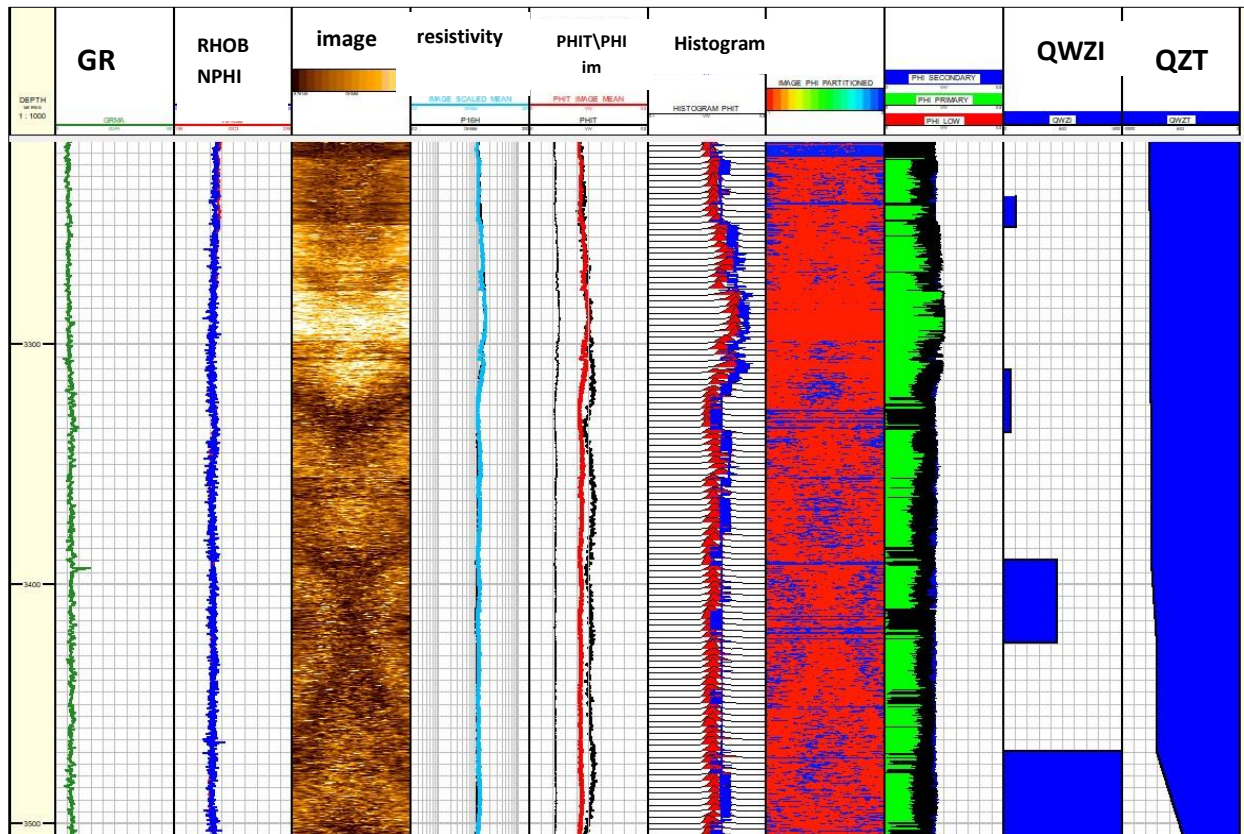


Fig. (5): The study well results the image porosity and the dynamic data (PLT).

Due to the heterogeneity at the carbonate rocks and for more understanding the image porosity analysis was applied to evaluate carbonate dual-porosity systems using borehole electrical images. This type of analysis likely involves the study of subsurface rock formations, particularly carbonate rocks, which can exhibit complex porosity characteristics due to both primary and secondary pore systems. Carbonate rocks often have a combination of matrix porosity (primary porosity) and fractures or vuggy porosity (secondary porosity). Borehole electrical imaging techniques are used to capture detailed images of the borehole wall, which can provide valuable insights into the distribution and characteristics of these porosity types. The PoroSpect technique is helpful to more understanding the carbonate reservoirs. The injection is mostly depending on the permeable zones whilst; the porosity values are so similarity at the horizontal's wells. These images reveal resistivity variations that correlate with different porosity types. Porosity Classification: Researchers or geologists analyze the images to identify different porosity types. The primary matrix porosity might appear as relatively to the depositional conditions, while

secondary porosity caused by the diagenesis such as fractures and vugs might be seen as irregular patterns. Water injection can reduce oil viscosity, facilitating improved flow toward production wells. Dedicated Injection and Production Wells: The drilling of dedicated injection and production wells is a common feature of a water injection project. Injection wells are used to inject water into the reservoir, whereas production wells are used to retrieve the oil and water mixture created during the injection operation. While water injection can help improve oil recovery, its success is reliant on a number of factors, such as reservoir characteristics, fluid properties, and overall injection process management. Water quality, injection rates, and pressure maintenance strategies are just a few of the aspects that must be taken into account for an effective water injection program. To better understand water injection, the high-resolution image log provides high-quality information about porosity types and the porosity distribution. The secondary porosity that results from diagenesis gives more understanding of where dissolution, fractures, and vugs are located. That helps to be empathetic about where injection water is taken and maintain the formation pressure. Furthermore, by using this technique to link injection zones with producer intervals at the producer wells, abrupt water cut increasing.

4. Conclusions

The PoroSpect technique, which is used in this manuscript, depends on converting the microresistivity log data to porosity. This technique is high-resolution data; the vertical resolution is 0.2" and covers the full-bore area. All conventional log information is low resolution (about 15.24") and represents 1D direction. The permeable zone, which absorbs the majority of the injection water, is more closely related to the secondary porosity. Even if the main porosity is greater than 20%, it is created by depositional processes unrelated to injection zones. The depiction of the injection zones corresponds well with the zones of significant secondary porosity (5-8%). In order to prevent a rise in water cuts at the producers' wells, this case study provides details on where the injection water is collected. The developed method allows for understanding the relationship between different carbonate porosity types and injection behavior. The current case study concludes that primary porosity does not account for full production. The porosity types reflect the injection patterns in the reservoirs. Secondary porosity contributes more significantly to injectivity than primary porosity. The current study, in spite of data limitation (horizontal PLT at the injector wells) but provide good results for the injection behavior with the secondary

porosity. This is critical for well completion, carrying out optimum completion, designing hydraulic fracturing stages, and placing packers and inflow control devices.

References

- [1] M. A. Abdulhameed, F. M. Al-Najm, and M. M. Mahdi, "Geometry and tectonic history of West Qurna-1 structure, Southern Iraq, Mauddud Carbonate Reservoir as case study", *The Iraqi Geological Journal*, vol. 57, no. 1E2, pp. 239-251, 2024. <https://doi.org/10.46717/igi.57.1E.15ms-2024-5-26>
- [2] A. A. M. Aqrabi, T. A. Mahdi, G. H. Sherwani, and A. D. Horbury, "Characterization of the mid-Cretaceous Mishrif reservoir of the southern Mesopotamian basin, Iraq", In *American Association of Petroleum Geologists Conference and Exhibition*, vol. 7, pp. 7-10, 2010.
- [3] S. Jasim, and J. Goff, "Geology of Iraq", *DOLIN*, printed in (Zech. Repub.), distributed by Geological Society of London, 2006.
- [4] P. R. Sharland, D. M. Casey, R. B. Davies, M. D. Simmons, and O. E. Sutcliffe, "Arabian plate sequence stratigraphy—revisions to SP2", *GeoArabia*, vol. 9, no. 1, pp. 199-214, 2004. <https://doi.org/10.2113/geoarabia0901199>
- [5] J. Lai, G. Wang, S. Wang, J. Cao, M. Li, X. Pang, C. Han, X. Fan, L. Yang, Z. He, and Z. Qin, "A review on the applications of image logs in structural analysis and sedimentary characterization", *Marine and Petroleum Geology*, vol. 95, pp. 139-166, 2018. <https://doi.org/10.1016/j.marpetgeo.2018.04.020>
- [6] J. Lai, K. Chen, Y. Xin, X. Wu, X. Chen, K. Yang, Q. Song, G. Wang, and X. Ding, "Fracture characterization and detection in the deep Cambrian dolostones in the Tarim Basin, China: Insights from borehole image and sonic logs", *Journal of Petroleum Science and Engineering*, vol. 196, p. 107659, 2021. <https://doi.org/10.1016/j.petrol.2020.107659>
- [7] S. E. Pinsky, "Advances in borehole imaging technology and applications", *Geological Society, London, Special Publications*, vol. 159, no. 1, pp. 1-43, 1999. <https://doi.org/10.1144/GSL.SP.1999.159.01.01>
- [8] M. Poppelreiter, C. Garcia-Carballido, and M. Kraaijveld, "Dipmeter and borehole image log technology", *AAPG Memoir 92*, vol. 92, 2010.
- [9] M. C. Muniz, and D. W. J. Bosence, "Pre-salt microbialites from the Campos Basin (offshore Brazil): image log facies, facies model and cyclicity in lacustrine carbonates", *Geological Society, London, Special Publications*, vol. 418, no. 1, pp. 221-242, 2015. <https://doi.org/10.1144/SP418.10>
- [10] M. E. J. Wilson, D. Lewis, O. K. Yogi, D. Holland, L. Hombo, and A. Goldberg, "Development of a Papua New Guinean onshore carbonate reservoir: a comparative borehole image (FMI) and petrographic evaluation", *Marine and Petroleum Geology*, vol. 44, pp. 164-195, 2013. <https://doi.org/10.1016/j.marpetgeo.2013.02.018>
- [11] M. J. Ismail, M. M. Mahdi, F. R. Etensohn, R. A. Abdullah, A. M. Handhal, and A. M. Al-Abadi, "High-resolution sequence stratigraphy and microfacies analysis of the lower part of the Sa'di Formation in selected wells from the West Qurna oilfield, southern Iraq", *Journal of African Earth Sciences*, vol. 228, p. 105639, 2025. <https://doi.org/10.1016/j.jafrearsci.2025.105639>
- [12] R. G. Maliva, E. A. Clayton, and T. M. Missimer, "Application of advanced borehole geophysical logging to managed aquifer recharge investigations", *Hydrogeology Journal*, vol. 17, no. 6, pp. 1547–1556, 2009. <https://doi.org/10.1007/s10040-009-0437-z>

- [13] M. Akbar, J. Steckhan, M. Tamimi, T. Zhang, and S. Saner, “Estimating cementation factor (m) for carbonates using borehole images and logs”, In *Abu Dhabi International Petroleum Exhibition and Conference SPE*, Nov. 2008. <https://doi.org/10.2118/117786-MS>
- [14] B. M. Newberry, L. M. Grace, and D. D. Stief, “Analysis of carbonate dual porosity systems from borehole electrical images”, In *SPE Permian Basin Oil and Gas Recovery Conference*, March 1996. <https://doi.org/10.2118/35158-MS>
- [15] R. A. Abdullah, K. Al-Jorany, F. Mohsin, A. Imad, and M. Abdulrazaq, “Edge Water Breakthrough in each of the major zones within Mishrif reservoir in West Qurna phase 1”, *Journal of Petroleum Research and Studies*, vol. 8, no. 3, pp. 79-96, Sep. 2018. <https://doi.org/10.52716/jprs.v8i3.253>
- [16] H. M. Shehhi, S. S. Shehab, R. I. Celma, S. Girinathan, and B. Sadaoui, (2016, November). “Well Productivity Analysis Integrating Ultra-High Resolution LWD Images and PLT: A Data Integration Case Study”, In *Abu Dhabi International Petroleum Exhibition and Conference*, Abu Dhabi, UAE, November 2016. <https://doi.org/10.2118/183463-MS>
- [17] M. Tadayoni, M. Khalilbeyg, and R. Bin Junin, “A new approach to heterogeneity analysis in a highly complex carbonate reservoir by using borehole image and conventional log data”, *Journal of Petroleum Exploration and Production Technology*, vol. 10, pp. 2613-2629, 2020. <https://doi.org/10.1007/s13202-020-00930-4>